

Short communication

Statistical Analysis of the Most Prominent Geoeffective Coronal Mass Ejections Associated with Intense Geomagnetic Storms in Solar Cycle 24

Abstract

A main contributor to space weather, geomagnetic storms especially intense ones, can severely affect space-borne and ground-based technological systems. Thus, it is important to investigate the geo-effective causes of storms at the Sun, and in the solar atmosphere. Geomagnetic storms are primarily caused by intense, long-duration, and southward interplanetary magnetic field (IMF) events, associated with intense and long-lasting interplanetary fields. In the present study, a total of 23 intense geomagnetic storms ($Dst \leq -100$ nT) have been found during the period of solar cycle 24 and used to represent the relationship between intense geomagnetic storms and solar activity parameters. One of the main solar phenomena is CMEs, when occurred earth directed, produce geomagnetic storms. It is also observed that these intense geomagnetic storms are associated with disturbances in solar wind plasma parameters. Positive correlation with a correlation coefficient of 0.48 has been found between the magnitude of intense geomagnetic storms and the peak value of IMF(B), 0.37 has been found between the magnitude of intense geomagnetic storms and the magnitude of IMF(B), 0.27 between the magnitude of intense geomagnetic storms and the peak value of associated disturbances in the southward component of IMF (B_z), 0.15 between the magnitude of intense geomagnetic storms and the peak value of associated disturbances in the southward component of IMF (B_z). Also, we have observed that out of 23 intense geomagnetic storms, 23 are associated with CMEs in which 14 (61%) halo CMEs and 9 (39%) partial halo CMEs occurred. Hence, we conclude that CMEs play a crucial role in geomagnetic storms.

Keywords- Coronal Mass Ejections (CMEs), Geomagnetic Storms (GMs), Disturbance Storm Time (Dst), Interplanetary Magnetic Field (IMF).

1. Introduction

The sun is a magnetic variable star that fluctuates on different time's scales. All solar activity is driven by the solar magnetic field. As the wind travels from the sun, it carries charged particles and magnetic

clouds emitted in all directions; some of the solar wind is constantly buffeting our magnetosphere, with interesting effects. The solar wind is a stream of energized charged particles, primarily electrons and protons, flowing outward from the Sun. Coronal Mass Ejections (CMEs) are large expulsions of plasma and magnetic field from the Sun's corona. Sunspot activity cycle occurs in approximate every eleven years^{4,5}. A geomagnetic storm is the consequence of a chain of causative events originating from the Sun and ultimately evolving into a geo-effective solar wind flow near earth space^{1,6}. From the results of the past three decades, it is confirmed that CMEs are large-scale magnetized plasma structures originating from closed magnetic field regions the sun: active regions, filament regions, active region complexes, and trans equatorial interconnecting regions⁵ and drive solar wind (SW) disturbances in terms of the magnetic field, speed and density, which in turn cause magnetic disturbance in the magnetosphere¹¹. It has been established by now that geomagnetic storms occur when the southward component of interplanetary magnetic field (IMF), B_z , impinges upon the Earth's magnetosphere and reconnects⁵. Several statistical observational studies have been done to investigate the properties of solar flares and/or CMEs. ¹² indicated that the risetime of the soft-X-ray flux of a flare is approximately half of the decay time, and the rise and decay times increase with variations in the peak flux of the soft X-ray. Regarding CMEs, ⁹ investigated the frequency distributions in the energy of solar flares and found that the power law indices of the frequency distributions for flares without CMEs are steeper than those for flares with CMEs. ⁸ have studied geomagnetic storms ($Dst < -100$ nT) observed during the period of 2014 -2017, with halo and partial halo coronal mass ejections associated with X-ray solar flares of different categories and concluded that they have concluded that majority of the observed geomagnetic storms are found that halo and partial halo CMEs associated with X ray solar flares are most potential candidates for production of geomagnetic storms. ⁷ have concluded that halo coronal mass ejections (H-CMEs) originating from regions close to the centre of the sun are likely to be geoeffective. They have showed that, only fast halo CMEs (with space velocities higher than ~ 1000 km/s) and originating from the Western Hemisphere close to the solar centre could cause intense geomagnetic storms. ^{6,10} has studied the role of halo and partial halo CMEs in producing geomagnetic storms. He has reviewed the results obtained by previous investigators and concluded that the generation of geomagnetic storms rates can be readily explained by the different definition of halo CMEs used by different authors. Partial halos are less energetic and generally originate far from the disk centre, so most of them behave similar to the non-geo-effective CMEs and hence most of the partial halo CMEs may not produce geomagnetic storms. He has inferred that halo CMEs originating close to the disk centre or very much effective in producing geomagnetic storms. Since coronal plasmas are heated to 10–20 MK during solar flares, the characteristics of solar flares are often identified

through X-ray observations. The magnitude of a solar flare is usually defined by the peak flux of the soft-X-ray measured by the Geostationary Operational Environmental Satellite (GOES) and classified into several classes (A, B, C, M, and X). In this investigation, we have studied intense geomagnetic storms associated with the foremost geo-effective coronal mass ejections during solar cycle 24.

Comment [Bs1]: Split this paragraph in three or four parts.

2. Methodology

Several solar and interplanetary phenomena, including coronal mass ejections and interplanetary magnetic fields, were studied using geomagnetic storms ($Dst < -100$) during solar cycle 24 (5). Various statistical approaches, such as association auto- and cross-correlation and curve-fitting regression, were used for this investigation. The omni-web data of the DST index was used in this paper to determine geomagnetic storms. SOHO (big angle spectrometric coronagraph) and extreme ultraviolet imaging telescope (SOHO/EIT) data are used to calculate coronal mass ejections (CMEs). For the data analysis of recorded geomagnetic storms with perturbations in interplanetary magnetic field data, this study uses statistical methods of association and correlation. In this paper, various solar and interplanetary phenomena such as coronal mass ejections, and interplanetary magnetic fields data have been analyzed with geomagnetic storms ($Dst \leq -100$) during solar cycle 24(5). For this analysis, different statistical methods such as association auto and cross correlation, curve fitting regression have been used. For this paper, the omni web data of Dst index have been used to determine geomagnetic storms. The data of coronal mass ejections (CMEs) is taken from SOHO— large angle spectrometric coronagraph (LASCO) and extreme ultraviolet imaging telescope (SOHO/EIT) data. This study uses statistical method association and correlation for data analysis of the observed geomagnetic storms with disturbances in interplanetary magnetic field data.

Comment [Bs2]: It is better if you briefly explain your methodology.

3. Data analysis and results

In this article, we observed 23 powerful geomagnetic storms (GMSs), i.e., $DST < -100$ nT, of which 23 coronal mass ejections are related with the CME catalog. In this paper, we have observed 23 geomagnetic storms (GMSs) which are of intense i.e., ($Dst \leq -100$ nT) have been selected, out of which 23 coronal mass ejections are found to be associated CME catalogue. As indicated in Fig 1, data analysis of geomagnetic storms and accompanying perturbations in interplanetary magnetic fields (B) was performed. All of the strong geomagnetic storms are connected with perturbations in interplanetary magnetic fields (B), with a lowest peak value of 4.2 nT to a highest peak value of 31.5 nT and a magnitude ranging from 3.7 nT to 23.7 nT. From the data analysis of geomagnetic storms and associated disturbances in interplanetary magnetic fields (B) is shown by (fig.1,2). It is observed that all the strong geomagnetic

storms are associated with disturbances in interplanetary magnetic fields (B) with lowest peak value 4.2nT to highest peak value 31.5nT and lowest magnitude 3.7 nT to highest magnitude 23.7 nT. The majority of greater-magnitude geomagnetic storms are associated with considerably higher peak-value perturbations in IMF (B). The trend line of the scatter plot between the magnitude of powerful geomagnetic storms and the peak value of IMF (B) shown in Fig. 1 and the magnitude of disturbances in IMF (B) shown in Fig. 2 reveals a positive correlation. Statistical methods revealed a positive correlation with a correlation coefficient of 0.48 between peak values of disturbances in the IMF (B) and the magnitude of strong geomagnetic storms and 0.37 between the magnitude of disturbances in the IMF (B) and the magnitude of strong geomagnetic storms (Loeweet et al. 1997). Most of the strong geomagnetic storms of higher magnitudes are associated with relatively higher peak value disturbances in IMF (B). The trend line of scatter plot between the magnitude of strong geomagnetic storms and the peak value of IMF (B) given in (fig. 1) and magnitude of strong geomagnetic storms and magnitude of disturbances in IMF (B) given in (fig. 2) shows positive correlation. A positive correlation with correlation coefficient 0.48 between peak values of disturbances in IMF (B) and magnitude of strong geomagnetic storms and 0.37 between the magnitude of disturbances in IMF (B) and magnitude of strong geomagnetic storms have been obtained by statistical methods (Loeweet al. 1997).

Comment [Bs3]: It is better if you use your references styles APA

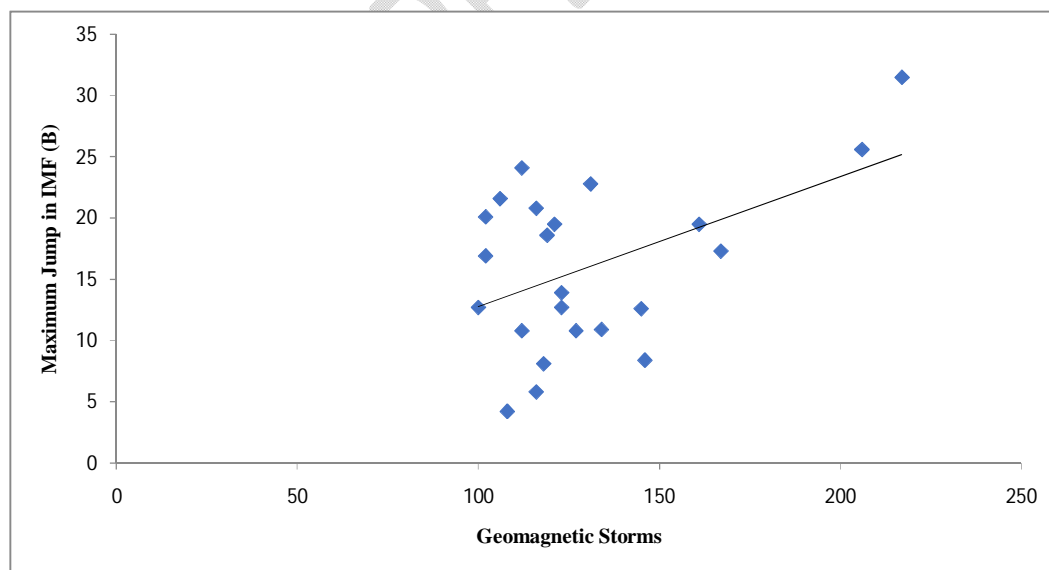


Fig. 1- Scatter plot between geomagnetic storms and maximum Jump in IMF (B)

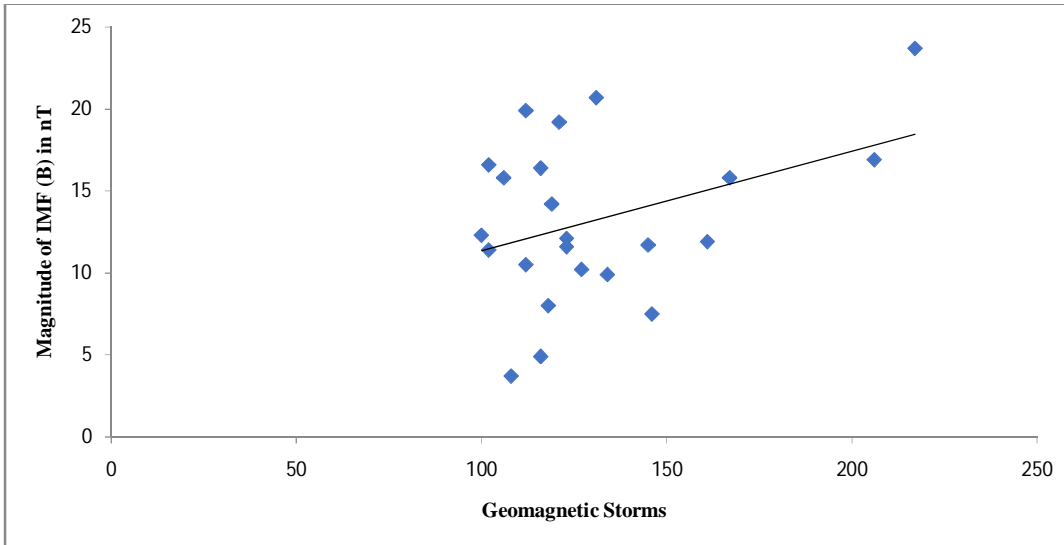


Fig. 2- Scatter plot between geomagnetic storms and magnitude of IMF (B)

Strong geomagnetic storms and related disturbances in a southerly component of interplanetary magnetic fields (Bz) as depicted in Figs. 3 and 4. All of the strong geomagnetic storms are associated with disturbances in the southward component of interplanetary magnetic fields (Bz) with the lowest peak value to the 7.6 nT to the highest peak value -26.3 nT and lowest magnitude 5.4 nT to the highest magnitude 24 nT. The scatter plot trend line between the size of intense geomagnetic storms and the jump in IMF (Bz) shown in Fig. 3 and the magnitude of severe geomagnetic storms and the amplitude of disturbances shown in Fig. 4 reveals a positive correlation. Statistical methods revealed a positive link with a correlation coefficient of 0.27 between peak values of disturbances in the IMF (Bz) and 0.15 between the magnitude of disturbances in the IMF (Bz) and the size of intense geomagnetic storms. From the data analysis of strong geomagnetic storms and associated disturbances in a southward component of interplanetary magnetic fields (Bz) shown in (fig. 3 and 4). It is observed that all the strong geomagnetic storms are associated with disturbances in the southward component of interplanetary magnetic fields (Bz) with lowest peak value -7.6 nT to highest peak value -26.3 nT and lowest magnitude 5.4 nT to highest magnitude 24 nT. The trend line of scatter plot between the magnitude of strong geomagnetic storms and the Jump in IMF (Bz) given in (fig. 3) and magnitude of strong geomagnetic

Comment [Bs4]: It is better if you split into two sentences

storms and magnitude of disturbances in IMF (Bz) given in (fig. 4) shows positive correlation. A positive correlation with correlation coefficient 0.27 between peak values of disturbances in IMF (Bz) and 0.15 between the magnitude of disturbances in IMF (Bz) and magnitude of intense geomagnetic storms obtain by statistical methods.

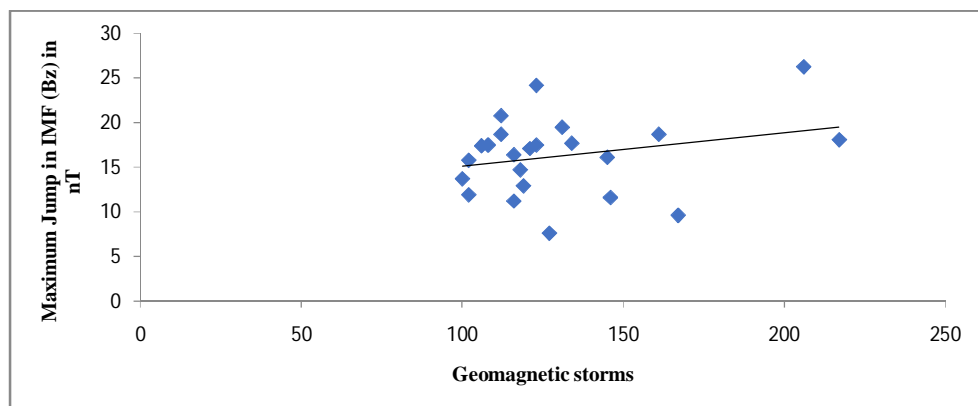


Fig. 3- Scatter plot between geomagnetic storms and maximum jump in IMF (Bz)

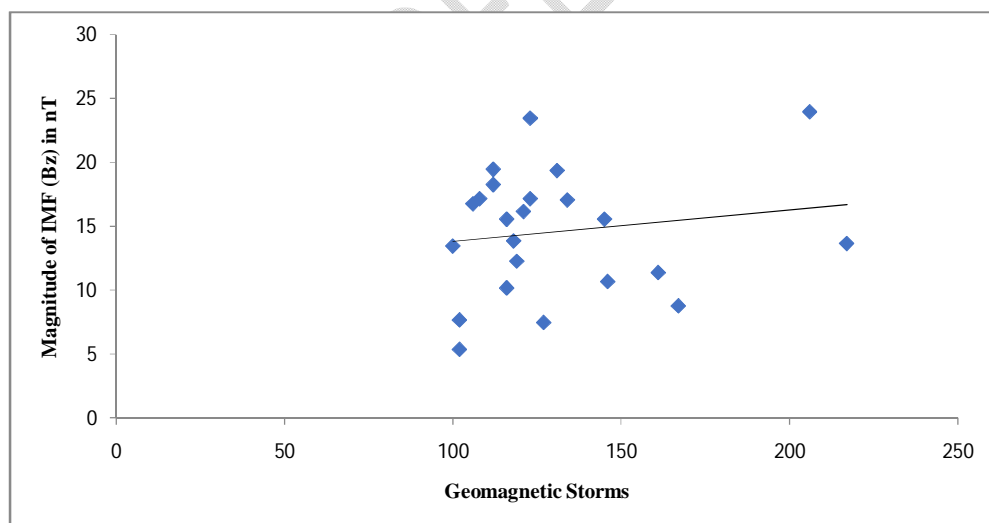


Fig. 4- Shown Scatter plot between magnitude of strong geomagnetic storms and magnitude of associated disturbances in IMF.

According to the data analysis of significant geomagnetic storms during solar cycle 24, 61% of HALO CMEs and 39% of partial HALO CMEs were caused by protracted proton events that occurred over the last several years, as shown in Fig. 5. From the data analysis of strong geomagnetic storms during the period of solar cycle 24, we have found 61% of HALO CMEs and 39% of Partial Halo CMEs due to prolonged proton events occurred due to the last several years which is shown in (fig. 5).

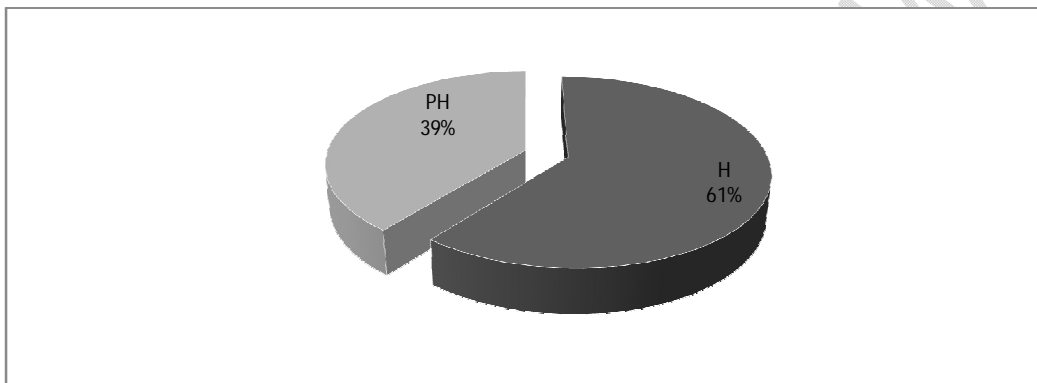


Fig. 5 Pie diagram of associated CMEs in percentage

4. Conclusion

During the solar cycle 24 period, 23 geomagnetic storms (GMSs) (Dst) were discovered in the current investigation. The following conclusions are obtained from data on geomagnetic storms and their association with the southern component of the interplanetary magnetic field (Bz), the interplanetary magnetic field (B), and coronal mass ejections: In present study, 23 geomagnetic storms (GMSs) (Dst ≤ -100) are found during the period solar cycle 24. On the basis of geomagnetic storms association with southward component of interplanetary magnetic field (Bz), interplanetary magnetic field (B) and coronal mass ejections data are analyzed with following conclusions:

1- The high-speed solar wind plasma may take the form of CMEs, or it may cause GMSs. As a result, VSW can be used to predict the strength of GMSs. The high-speed solar wind plasma may be in the form of CMEs or else is more likely to cause the GMSs. Hence, VSW may be taken as a reliable indicator of strength of GMSs.

2- There is no correlation between storm duration and the quantity of CMEs involved in its occurrence. The number of CMEs that cause the storm to occur has little effect on the strength of the GMSs. ~~No relationship is observed between storm duration and the number of CMEs involved in its occurrence. The intensity of the GMSs is also independent of the number of CMEs causing the occurrence of the storm.~~

3- The IMF (B) value in GSE coordinates has a superior association and a high positive correlation with the DST index. Statistical methods revealed a positive correlation with a correlation coefficient of 0.48 between peak values of disturbances in IMF (B) and the magnitude of strong geomagnetic storms, as well as a correlation coefficient of 0.37 between the magnitude of disturbances in IMF (B) and the magnitude of strong geomagnetic storms. ~~The IMF (B) value in GSE coordinates shows better relationship with Dst index and shows a strong positive correlation. A positive correlation with correlation coefficient 0.48 between peak values of disturbances in IMF (B) and magnitude of strong geomagnetic storms and 0.37 between the magnitude of disturbances in IMF (B) and magnitude of strong geomagnetic storms have been obtained by statistical methods.~~

4- The IMF (Bz) value in GSE coordinates has a superior association and a high positive correlation with the DST index. Statistical methods revealed a positive correlation with a correlation coefficient of 0.27 between peak values of disturbances in the IMF (Bz) and the magnitude of strong geomagnetic storms and 0.15 between the magnitude of disturbances in the IMF (Bz) and the magnitude of strong geomagnetic storms. ~~The IMF (Bz) value in GSE coordinates shows better relationship with Dst index and shows a strong positive correlation. A positive correlation with correlation coefficient 0.27 between peak values of disturbances in IMF (Bz) and magnitude of strong geomagnetic storms and 0.15 between the magnitude of disturbances in IMF (Bz) and magnitude of strong geomagnetic storms have been obtained by statistical methods~~

5- 61% of HALO CMEs are responsible for the strong geomagnetic storms.

References

1. Brueckner, G. E., Howard, R. A., Koomen, M. J., Korendyke, C. M., Michels, D. J., Moses, J. D. The Large Angle Spectroscopic Coronagraph (LASCO), Solar Physics, Vol. 162, (1995), 357.
2. Benz, A. O. Flare observations. LRSP, 14, (2017), 2.
3. Gopalswamy N., Coronal Mass Ejections of Solar Cycle 23, J. Astrophys. Astr, 27,(2006), 243.

4. Gopalswamy N., Yashiro S and Akiyama S., Geoeffectiveness of halo coronal mass ejections, *Journal of Geophysical Research*, (2007), 112.
5. Gopalswamy N, Yashiro, Y. Liu, G. Michalek, A. Vourlidas, M. L. Kaiser, R. A. Howard, Coronal mass ejections and other extreme characteristics of the 2003 October–November solar eruptions, (2003), <https://doi.org/10.1029/2004JA010958>.
6. Gopalswamy, N., Halo coronal mass ejections and geomagnetic storms. *Letter Earth Planets Space*, 61, (2009). 1.
7. Michalek, G., Gopalswamy, N., Lara, A., and Yashiro. Properties and geo-effectiveness of halo coronal mass ejections. *Space Weather*, (2006), 4.
8. Pandey, V., Kumar, S., Ochani, D., Verma, P. L. H-CMEs and solar wind plasma disturbances in relation to intense geomagnetic storms during the period of 2014-2017. *Int J Innovat Res Growth*, 11, (2022), 28.
9. Yashiro, S., Gopalswamy, N., Michalek, G., A catalog of white light coronal mass ejections observed by the SOHO spacecraft 2004. *JGRA*, 109, (2004), 07105.
10. Zhang, J., Dere, K. P., Howard, R. A., Kundu, M. R., & White, S. M., (2001). On the temporal relationship between coronal mass ejections and flares, *ApJ*, 559, 452.
11. Zhang, J., Dere, K. P., Howard, R. A., and Bothmer, V., Identification of Solar Sources of Major Geomagnetic Storms between 1996 and 2000, *The Astrophys. J.* 582, (2003). 520.
12. Zhang, P., & Liu, S.-M., Statistical Relation between Solar Flares and Coronal Mass Ejections with Respect to Sigmoidal Structures in Active Regions, *ChA&A*, 39, (2015), 330.